ELSEVIER

Inorganica Chimica Acta 340 (2002) 147–154

Inorganica Chimica Acta

www.elsevier.com/locate/ica

# The effects, assessed by electrochemical techniques and single crystal structures, of *ortho* substitution on benzoate ligands supporting the quadruply-bonded dimolybdenum bond

Teerayuth Liwporncharoenvong, Rudy L. Luck *

*Department of Chemistry, Michigan Technological University, 1400 Townsend Drive, Houghton, MI 49931, USA*

Received 20 February 2002; accepted 7 May 2002

## Abstract

The syntheses, electrochemistry and structures of $Mo_2(O_2C\text{-}o\text{-}C_6H_4Cl)_4$, **1**·4THF, $Mo_2(O_2C\text{-}o\text{-}C_6H_4Br)_4$, **2**·2THF, $Mo_2(O_2C\text{-}o\text{-}C_6H_4I)_4$, **3**·2THF, and $Mo_2(O_2C\text{-}o\text{-}C_6H_4NO_2)_4$ (**4**), as determined by single-crystal X-ray diffraction, are reported. Molecules **1**, **2**, and **3** co-crystallized each with two axially coordinated THF molecules; complex **1** contained two more THF molecules within the unit cell. The Mo–Mo distances in **1**–**4** are 2.1029(10), 2.1014(13), 2.1055(7), and 2.0942(12) Å, respectively. The oxidation potentials for **1**–**3** were similar at 674, 655, and 647 mV, but that for **4** at an $E_{1/2}$(ox) of 792 mV was higher.

*Keywords:* Electrochemical techniques; Benzoate ligands; Quadruply-bonded dimolybdenum

## 1. Introduction

The tetracarboxylato dimolybdenum(II) unit is well established [1] and various carboxylate ligands have been employed to stabilize the $Mo_2^{4+}$ core unit, e.g. $Mo_2(O_2CCF_3)_4$ [2], $Mo_2(O_2CC_6H_5)_4$ [3], $[Mo_2(O_2CCH_2NH_3)_4]Cl_4 \cdot 3H_2O$ [4] and $Mo_2(FCA)_4(NCCH_3)(DMSO) \cdot 2DMSO$ [5] (FCAH = ferrocenemonocarboxylic acid). An examination [3] consisting of variance on axial coordination and inductive effects of the ligand, found that the Mo–Mo quadruple bond was not sensitive and compared with the $Cr_2^{4+}$ core [6] resisted change.

We were interested in a consideration of both ligand-inductive effects and $Mo_2^{4+}$ consequence by use of *o*-substituted benzoic acid derivatives. There appears to be only two such compounds established structurally, i.e. $Mo_2(O_2CC_6H_4\text{-}o\text{-}C_6H_5)_4$ [7] and $Mo_2(O_2CC_6H_4\text{-}o\text{-}OH)_4$ [8]. The ligands employed in this study were *o*-chloro, *o*-bromo, *o*-iodo, *o*-nitro-benzoic acids. It was of interest to see if the interplanar angles between the benzene and carboxylate groups would change upon coordination to the $Mo_2^{4+}$ core and if there would be any relationship between the degree of twist and the Mo–Mo atom interaction as assessed through crystallographic and electrochemical measurements.

## 2. Experimental

### 2.1. General data

Oxygen was excluded during all operations by using vacuum lines or a glovebox supplied with purified nitrogen. All solvents except methanol and water were dried over and distilled from sodium benzophenone ketyl. Methanol was dried over Magnesium metal. Water and all solvents were degassed before use. IR spectra were recorded by using a Mattson Galaxy Series FTIR 3000. NMR spectra were recorded on a Varian Unity Inova 400 mHz. Visible absorption spectra were recorded by using a Hewlett Packard 8452A diode array spectrophotometer. The preparation of $K_4Mo_2Cl_8$ was reported elsewhere [9]. Elemental analyses were obtained at Galbraith Laboratories, Inc., Knoxville, TN.

---

* Corresponding author. Tel.: +1-906-487 2309; fax: +1-906-487 2061

*E-mail address:* rluck@mtu.edu (R.L. Luck).

0020-1693/02/$ - see front matter © 2002 Elsevier Science B.V. All rights reserved.
PII: S0020-1693(02)01095-2

The electrochemical measurements were accomplished with a Bioanalytical Systems CV-50W workstation controlled by a 366 MHz Pentium based Gateway PC. The cyclic voltammetric experiments were performed in a 5.0 ml cell equipped with a glassy carbon working electrode (0.071 $cm^2$), a platinum wire auxiliary electrode, and a Ag/AgCl reference electrode. The electroactive compounds were dissolved (0.001 mol $l^{-1}$) in dried benzonitrile also containing tetrabutylammonium hexafluorophosphate (Fluka, >99%) as the supporting electrolyte (0.10 mol $l^{-1}$). An argon atmosphere was maintained over the solutions throughout the electrochemical experiments. Ferrocene oxidized at 0.51 V under these conditions.

## 2.2. Synthesis

### 2.2.1. Preparation of $Mo_2(C_7H_4O_2Cl)_4$ (**1**)

A solution of $K_4Mo_2Cl_8$ (200 mg, 0.317 mmol) in 10 ml of distilled water was added to a solution of *o*-chlorobenzoic acid (210 mg, 1.342 mmol) in 20 ml methanol. The yellow product was isolated by filtration and vacuum dried. Subsequent recrystallization with THF–hexanes resulted in compound **1**. Yield 220 mg, 85.60%; IR 1569 m, and 1506 versus $cm^{-1}$; $^1H$ NMR ($CDCl_3$) $\delta$ 7.32–7.40 (m, 8H), 7.46–7.49 (m, 4H), 8.16–8.19 (m, 4H); UV 424 nm (in THF). *Anal*. Calc. for $Mo_2C_{28}H_{16}O_8Cl_4$: C, 41.31; H, 1.98. Found C, 40.68; H, 2.05%.

### 2.2.2. Preparation of $Mo_2(C_7H_4O_2Br)_4$ (**2**)

A solution of $K_4Mo_2Cl_8$ (200 mg, 0.317 mmol) in 10 ml of distilled water was added to a solution of *o*-bromobenzoic acid (270 mg, 1.344 mmol) in 20 ml methanol. The solution was stirred under $N_2$ for at least 30 min. The resulting yellow product was isolated by filtration and vacuum dried. Subsequent recrystallization with THF–hexanes resulted in compound **2**. Yield 270 mg, 86.04%; IR 1567 m, and 1513 s $cm^{-1}$; $^1H$ NMR ($CDCl_3$) $\delta$ 7.27 (t, $J=2$ Hz, 4H), 7.38 (t, $J=2$ Hz, 4H), 7.68 (d, $J=2$ Hz, 4H), 8.14 (d, $J=2$ Hz, 4H); UV 424 nm (in THF). *Anal*. Calc. for $Mo_2C_{28}H_{16}O_8Br_4 \cdot C_4H_8O$: C, 36.12; H, 2.27. Found C, 37.26; H, 2.64%.

### 2.2.3. Preparation of $Mo_2(C_7H_4O_2I)_4$ (**3**)

A solution of $K_4Mo_2Cl_8$ (200 mg, 0.317 mmol) in 10 ml of distilled water was added to a solution of *o*-iodobenzoic acid (330 mg, 1.331 mmol) in 20 ml methanol. The solution was stirred under $N_2$ for at least 30 min. The powdery yellow product, which precipitated almost immediately, was filtered through a sintered-glass frit, and vacuum dried. Subsequent recrystallization with THF–hexanes resulted in compound **3**. Yield 337 mg, 90.27%; IR 1560 m, and 1497 s $cm^{-1}$; $^1H$ NMR ($CDCl_3$) $\delta$ 7.11 (t, $J=2$ Hz, 4H), 7.44 (t, $J=2$ Hz, 4H), 8.02 (d, $J=2$ Hz, 4H), 8.16 (d, $J=2$ Hz, 4H); UV 424 nm (in THF). *Anal*. Calc. for $Mo_2C_{28}H_{16}O_8I$: C, 28.50; H, 1.37. Found: C, 28.15; H, 1.61%.

### 2.2.4. Preparation of $Mo_2(C_7H_4NO_4)_4$ (**4**)

A solution of $K_4Mo_2Cl_8$ (200 mg, 0.317 mmol) in 10 ml of distilled water was added to a solution of *o*-nitrobenzoic acid (220 mg, 1.317 mmol) in 20 ml methanol. The solution was stirred under $N_2$ for at least 30 min. The powdery red product was filtered through a sintered-glass frit, and vacuum dried. Subsequent recrystallization with THF–hexanes resulted in compound **4**. Yield 250 mg, 91.95%; IR 1605 m, 1519 versus, and 1400 s $cm^{-1}$; $^1H$ NMR ($CDCl_3$) $\delta$ 7.59 (t, $J=2$ Hz, 4H), 7.73 (t, $J=2$ Hz, 4H), 7.85 (d, $J=2$ Hz, 4H), 8.32 (d, $J=2$ Hz, 4H); UV 464 and 362 nm (in THF). *Anal*. Calc. for $Mo_2C_{28}H_{16}N_4O_{16}$**:** C, 39.27; H, 1.88. Found: C, 38.43; H, 1.94%.

## 2.3. Crystallography

In all cases, crystals were removed from the mother liquor, coated with epoxy resin and placed on the head of a thin glass fiber, which was anchored in a goiniometer mounting pin. The pin-mounted crystal was then inserted into the goniometer head of the X-ray diffractometer and centered in the beam path. Standard CAD4 centering, indexing, and data collection programs were utilized [10]. About 25 reflections between 10 and 15° in $\theta$ were located by a random search pattern, centered and used in indexing. Final cell constants and orientation matrix were obtained by collecting appropriate preliminary data and refined by a least-squares fit. During data collection, three intensity standards and three orientation standards were measured at regular intervals to measure the rate of decay of the crystal and to accommodate for crystal movement.

Data were first reduced and corrected for absorption using psi-scans [11] and then solved using the program SIR-97 [12], which afforded nearly complete solutions for the non-H atoms in all cases. These programs were utilized using the WINGX interface [13]. The models were then refined using SHELXL-97 [14] first with isotropic and then anisotropic thermal parameters to convergence. The positions and isotropic thermal parameters of H-atoms were constrained and set to 1.5 times the isotropic equivalent of the atoms they were attached to, respectively. This constituted the final model for both compounds and appropriate crystallographic data is listed in Table 1. In **1** there were disorder in one of the THF molecules of solvation and in **4**, one of the oxygen atoms on the nitro groups on each unique molecule was disordered. Attempts to model Cl atoms at the same site as the Br atoms in **2** or constrained at separate distances were not successful as no significant deviation away from unity for the Br occupancy was observed in

Table 1
Crystal data and structure refinement details for **1**–**4**

| | **1**·4THF | **2**·2THF | **3**·2THF | **4** |
|---|---|---|---|---|
| Formula | $C_{28}H_{16}Mo_2O_8Cl_4\cdot 4C_4H_8O$ | $C_{28}H_{16}Mo_2O_8Br_4\cdot 2C_4H_8O$ | $C_{28}H_{16}Mo_2O_8I_4\cdot 2C_4H_8O$ | $C_{56}H_{32}Mo_4O_{32}N_8$ |
| $M_r$ | 1102.55 | 1136.14 | 1324.14 | 856.33 |
| Habit | yellow prism | yellow prism | yellow prism | red prism |
| Crystal system | orthorhombic | triclinic | monoclinic | triclinic |
| Space group | *Pbca* | $P\bar{1}$ | $P21/c$ | $P\bar{1}$ |
| $a$ (Å) | 9.4383(16) | 8.128(2) | 9.5680(11) | 11.018(3) |
| $b$ (Å) | 21.520(4) | 11.000(2) | 14.4670(14) | 11.800(2) |
| $c$ (Å) | 23.624(7) | 11.5170(15) | 14.8480(15) | 13.1884(18) |
| $\alpha$ (°) | 90 | 101.499(13) | 90 | 109.069(13) |
| $\beta$ (°) | 90 | 97.904(18) | 98.828(9) | 99.291(16) |
| $\gamma$ (°) | 90 | 100.275(19) | 90 | 103.092(18) |
| $V$ (Å$^3$) | 4798.3(18) | 976.7(4) | 2030.9(4) | 1525.9(5) |
| $\lambda$ (Mo K$\alpha$ radiation) | 0.71069 | 0.71069 | 0.71069 | 0.71069 |
| Temperature (K) | 293 | 293 | 293 | 293 |
| $Z$ | 4 | 1 | 2 | 2 |
| $D_{calc}$ (g cm$^{-3}$) | 1.53 | 1.93 | 2.17 | 1.86 |
| Number of reflctionns measured | 3127 | 2644 | 3582 | 5350 |
| Number of observed data $\lvert I\rvert > 2\sigma(I)$ | 2215 | 1798 | 3084 | 3035 |
| Number of parameters | 277 | 236 | 235 | 471 |
| $R_{int}$ | 0.078 | 0.096 | 0.038 | 0.113 |
| $R(F)$ [a] | 0.041 | 0.040 | 0.030 | 0.039 |
| $wR(F^2)$ [b] | 0.113 [c] | 0.072 [d] | 0.073 [c] | 0.072 [d] |
| Goodness-of-fit | 0.946 | 0.978 | 1.045 | 0.956 |
| Max. ($\Delta/\sigma$) | 0.005 | 0.001 | 0.001 | 0.001 |
| Residual max/min ($\Delta Q$) (e Å$^{-3}$) | 0.66/−0.34 | 0.57/−0.57 | 1.73/−1.33 | 0.80/−0.38 |

Scattering factors from international tables for crystallography (vol. C).
[a] $R = \Sigma(F_o - F_c)/\Sigma(F_o)$.
[b] $R_w = [\Sigma[w(F_o^2 - F_c^2)^2]/\Sigma[w(F_o^2)^2]]^{1/2}$.
[c] $w = 1/[\sigma^2(F_o^2) + (0.0434P)^2 + 0.5955P]$, where $P = (\max(F_o^2, 0) + 2F_c^2)/3$.
[d] $w = 1/[\sigma^2(F_o^2) + (0.0246P)^2 + 0.4445P]$, where $P = (\max(F_o^2, 0) + 2F_c^2)/3$.

the refinements. Selected bond distance and angles for **1**–**4** are given in Table 2.

## 3. Results and discussion

### 3.1. Synthetic and electrochemical details

Complexes **1**–**4** were prepared using slight adaptations to well established procedures [15] and their IR, $^1$H NMR and visible spectra are listed in the experimental section. These measurements confirmed the presence of the ligand, that the samples were diamagnetic and possessed an absorption in the visible previously assigned to a $\delta \rightarrow \delta^*$ transition [1].

Electrochemical studies on these compounds are of interest. The reversibility and quasi-reversibility of the $Mo_2^{4+}$ core in different solvents were previously noted [16]. Recently benzonitrile was used for electrochemical studies on dimolybdenum systems due to its high dielectric constant [17]. In this solvent, $Mo_2(acetate)_4$ exhibited a reversible oxidation at $E_{1/2} = 448$ mV ($\Delta E_p = 66$ mV) [18].

In this electrochemistry study, all four dimolybdenum complexes were measured in benzonitrile. Fig. 1 displays the voltammograms obtained at various scan rates using a glassy carbon electrode for **1**–**4**, with the data from these listed in Table 3. Compounds **1**–**3** appear to exhibit reversible voltammograms as evidenced by the fact that the $i_{pc}/i_{pa}$ ratio is 'close' to unity. However, under the measurement conditions, **4** exhibits quasi-reversible voltammograms as the $i_{pc}/i_{pa}$ deviates significantly from unity and with an $E_{1/2}(ox) = 780$ mV is the most difficult complex to oxidize.

Table 4 lists data for various dimolybdenum tetrabenzoate systems. There is a trend between p$K_a$ values and the oxidation potentials, i.e. the lower the p$K_a$ value, the higher the oxidation potential as we reported before [20]. The lower p$K_a$ values for the carboxylate ligands suggest that these ligands would donate less electron density to the $Mo_2^{4+}$ core rendering this unit harder to oxidize. It remains for additional studies in different solvents to determine the relationship between oxidation potentials and axial ligation.

### 3.2. Structural details

ORTEP3 FOR WINDOWS [22] representations of **1**–**4** are displayed in Figs. 2–5, respectively. In all cases, the molecules, including the two comprising **4**, see Fig. 5,

Table 2
Selected bond distance (Å) and angles (°) for **1**–**4**

| | **1** | **2** | **3** | **4** [a] |
|---|---|---|---|---|
| *Bond distances* | | | | |
| Mo1–Mo1 [b] | 2.1029(10) | 2.1014(13) | 2.1055(7) | 2.0942(12) |
| Mo1–O11 | 2.107(4) | 2.115(4) | 2.106(3) | 2.099(4) |
| Mo1–O12 [b] | 2.110(4) | 2.105(4) | 2.115(3) | 2.093(4) |
| Mo1–O21 | 2.111(4) | 2.122(4) | 2.103(3) | 2.134(3) |
| Mo1–O22 | 2.119(4) | 2.105(4) | 2.113(3) | 2.101(3) |
| O11–C10 | 1.264(7) | 1.270(8) | 1.274(5) | 1.271(6) |
| O12–C10 | 1.271(7) | 1.278(7) | 1.272(5) | 1.257(6) |
| O21–C20 | 1.275(7) | 1.260(8) | 1.278(5) | 1.271(6) |
| O22–C20 [b] | 1.262(7) | 1.276(7) | 1.273(5) | 1.261(6) |
| X1–C16 | 1.726(7) (X = Cl) | 1.911(8) (X = Br) | 2.101(4) (X = I) | 1.483(8) (X = N) |
| X2–C26 | 1.725(8) (X = Cl) | 1.868(9) (X = Br) | 2.102(5) (X = I) | 1.461(8) (X = N) |
| *Bond angles* | | | | |
| Mo1–Mo1–O11 [b] | 91.73(11) | 91.83(14) | 91.14(7) | 91.58(11) |
| Mo1–Mo1–O12 [b] | 91.56(11) | 91.55(12) | 91.10(8) | 92.05(11) |
| Mo1–Mo1–O21 [b] | 92.30(11) | 90.77(13) | 92.39(7) | 91.50(10) |
| Mo1–Mo1–O22 [b] | 90.84(11) | 92.18(13) | 91.02(7) | 92.21(10) |
| O11–Mo1–O21 | 88.76(16) | 89.21(17) | 91.14(11) | 90.71(14) |
| O11–Mo1–O22 | 90.59(15) | 90.59(17) | 88.52(11) | 90.53(14) |
| O12–Mo1–O21 [b] | 90.96(16) | 90.65(17) | 88.62(11) | 89.42(14) |
| O12–Mo1–O22 [b] | 89.50(15) | 89.37(17) | 91.52(11) | 89.11(14) |
| O11–Mo1–O12 [b] | 176.71(15) | 176.62(18) | 176.53(10) | 176.36(14) |
| O21–Mo1–O22 | 176.81(15) | 177.05(18) | 176.58(10) | 176.05(14) |
| Mo1–O11–C10 | 117.1(4) | 117.1(4) | 116.5(2) | 116.3(4) |
| Mo1–O12–C10 [b] | 116.9(4) | 117.7(5) | 117.3(2) | 116.4(3) |
| Mo1–O21–C20 | 116.8(4) | 118.3(4) | 116.8(3) | 115.5(3) |
| Mo1–O22–C20 [b] | 118.0(4) | 117.4(4) | 117.7(2) | 116.8(4) |
| O12–C10–C11 | 116.9(6) | 117.1(7) | 119.6(4) | 119.3(5) |
| O11–C10–O12 | 122.6(6) | 121.7(6) | 122.6(4) | 123.5(5) |
| O11–C10–C11 | 120.4(6) | 121.2(6) | 117.8(4) | 117.1(5) |
| O22–C20–O21 | 120.2(6) | 117.9(7) | 122.0(4) | 123.6(5) |
| C10–C11–C16 | 123.8(6) | 125.8(8) | 124.5(4) | 122.8(5) |
| C20–C21–C26 | 124.7(6) | 125.5(7) | 125.0(4) | 121.0(5) (X = N) |
| X1–C16–C11 | 122.7(5) (X = Cl) | 123.1(6) (X = Br) | 123.2(3) (X = I) | 119.7(5) (X = N) |
| X2–C26–C21 | 121.2(6) (X = Cl) | 124.6(6) (X = Br) | 123.8(3) (X = I) | 119.7(6) (X = N) |

[a] Distances and angles listed for only one molecule of **4**.

[b] Symmetry transformations used to generate equivalent atoms: $-x+1$, $-y$, $-z+1$.

were arranged around inversion points with one Mo atom and two complete ligands constituting the asymmetric unit, as is normally the case for similar molecules [23]. Compounds **1**–**3** each co-crystallized with two axially bound THF molecules and **1** contained two more THF molecules packed in a disordered arrangement (atoms refined with isotropic thermal parameters with restraints on the distances) in the void between the molecules in the unit cell. This resulted in the formulations given in Table 1. The fact that **4** does not possess any ligands bonded axially is the reason why the Mo–Mo atom distances at 2.0943(10) and 2.0963(10) Å for the two molecules is significantly shorter than the corresponding distance in **1**–**3** at 2.1029(10), 2.1014(13) and 2.1055(7) Å, respectively.

Table 5 lists the data for the interplanar carboxy–benzene angles for the free ligand and that of the corresponding dimolybdenum complex. It was previously established that as the size of the *o*-halogen substituent increased from F, Cl to Br, there was an increase in this angle assessed at 6.7, 13.7 and 18.3°, respectively [24]. This trend was not maintained with *o*-iodobenzoic acid which had an interplanar angle of 16.5(4)°, see Table 5. The reason for this, as the data in Table 5 illustrate, is that the dipole–dipole interactions between the halogen and carbonyl oxygen atoms are minimized both by increasing this interplanar angle as well as by the increase in the halogen–carbon atom bond distance (see Table 5), from Cl to I. Further, upon coordination of the acid ligands to the $Mo_2^{4+}$ core, we find the ligand maintains the same trend regarding the distances labeled as f and g in the diagram in Table 5, i.e. these distances increase from Cl to I. However, the corresponding interplanar angles for the Cl derivative **1** is more than twice that for the Br compound **2** and identical to that for the iodo **3**.

It is noteworthy that within compounds **1**, **3** and **4**, there were great differences in the same interplanar

Table 3
Visible spectra and electrochemical data for **1**–**4**

| Complex | MW | UV–Vis [b] | SR [c] | $E_{pc}$ (mV) | $E_{pa}$ (mV) | $E_{1/2}$ (mV) | $\Delta E_p$ (mV) | $i_{pc}$ (μA) | $i_{pa}$ (μA) | $(i_{pc}/i_{pa})$ [a] |
|---|---|---|---|---|---|---|---|---|---|---|
| **1** | 813.88 | 424 | 100 | 631 | 706 | 674 | 75 | 6.68 | 8.88 | 0.75, 0.85, 0.88 |
| **2** | 991.48 | 424 | 100 | 611 | 690 | 654 | 79 | 7.95 | 10.25 | 0.76, 0.83, 0.88 |
| **3** | 1179.48 | 424 | 100 | 606 | 686 | 646 | 80 | 9.99 | 11.49 | 0.87, 0.89, 0.91 |
| **4** | 859.88 | 362, 464 | 100 | 739 | 821 | 780 | 82 | 4.28 | 8.08 | 0.53, 0.58, 0.49 |

Values for all complexes are listed at scan rates of 100, 500, and 1000 mV $s^{-1}$, respectively.

[a] Electrochemical data are listed using notation in reference [19].

[b] nm, THF.

[c] BAS CV 50 electrochemical analyzer, SR, scan rate, glassy carbon working electrode, a platinum wire auxiliary electrode, a Ag/AgCl reference electrode, 0.001 mol $l^{-1}$ tetrabutylammonium hexafluorophosphate in dried benzonitrile as supporting electrolyte (0.10 mol $l^{-1}$), ferrocene oxidized at 510 mV under these conditions.

Table 4
Listing of oxidative potentials and Mo–Mo distance for various $Mo_2(O_2CR)_4$ compounds and the p$K_a$ values for the corresponding acids

| *R* | p$K_a$ [a] | $E_{1/2}$ (ox) (mV) | Mo–Mo distance (Å) | Working electrode, solvent |
|---|---|---|---|---|
| 2-$(NO_2)C_6H_4$ | 2.18 | 792 | 2.0942(7) | GCE, benzonitrile [b] |
| 2-$BrC_6H_4$ | 2.85 | 647 | 2.1014(13) | GCE, benzonitrile [b] |
| 2-$IC_6H_4$ | 2.86 | 655 | 2.1055(12) | GCE, benzonitrile [b] |
| 2-$ClC_6H_4$ | 2.88 | 674 | 2.1029(10) | GCE, benzonitrile [b] |
| 2,4,6-$(CH_3)_3C_6H_2$ | 3.44 | 610 | | GCE, benzonitrile [c] |
| 2,6-$(CH_3)_2C_6H_3$ | 3.36 | 570 | | GCE, benzonitrile [c] |

[a] These are the p$K_a$ values for the corresponding carboxylic acids in water at 25 °C [21].

[b] $E_{1/2}$ measured in this study.

[c] All data obtained from reference [17].

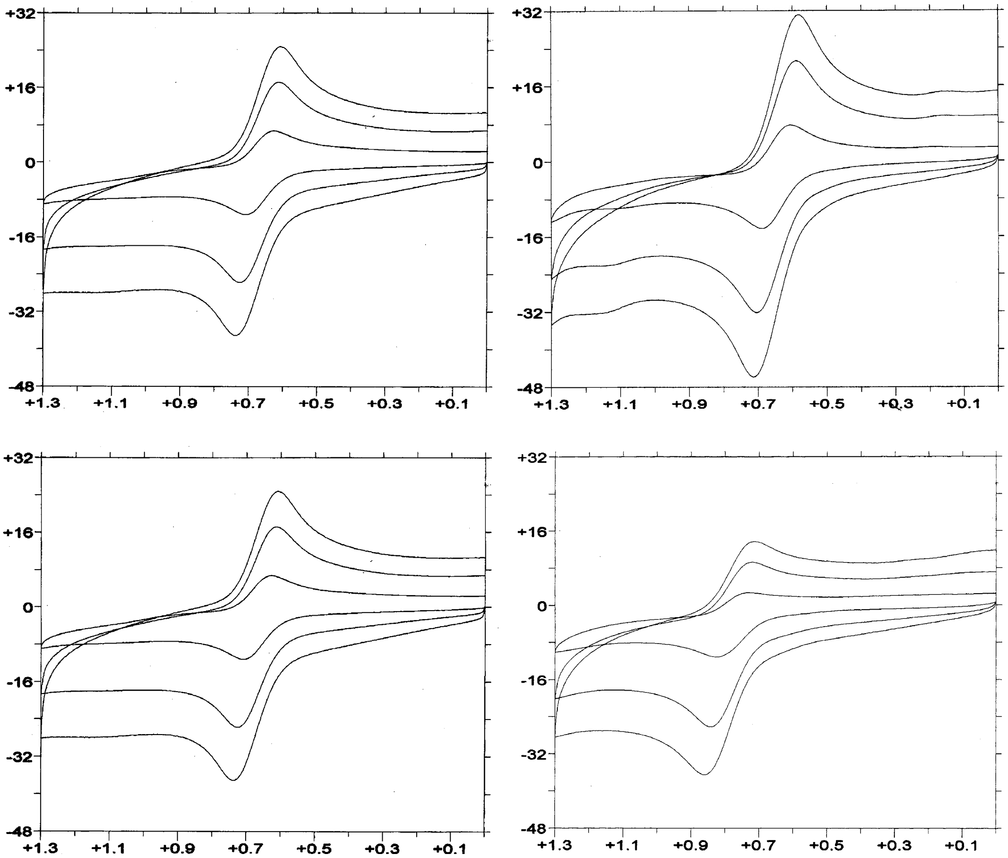

Fig. 1. Cyclic voltammogram plots at varying scan rates for **1**—top left, **2**—bottom left, **3**—top right, and, **4**—bottom right. Scan rates: 0.100 outer-; 0.500 middle-; and 1.000 inner-trace in V $s^{-1}$.

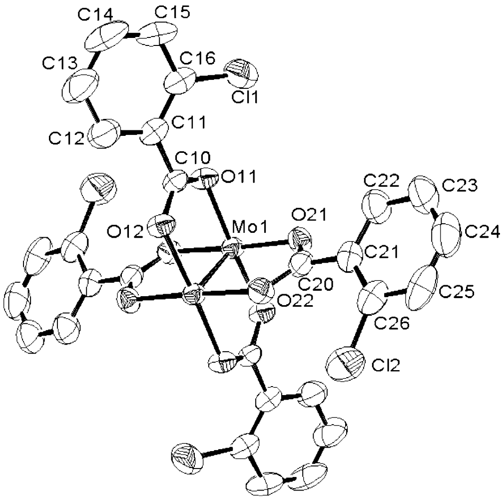

Fig. 2. ORTEP3 [22] representation of **1** displaying the atomic labeling scheme. THF molecules and H atoms were omitted for clarity. Thermal ellipsoids are drawn at the 50% probability level.

carboxy–benzene angle as the data in Table 5 illustrates. It was only in the bromo-derivative **2** that these angles at 13.8(6) and 15.1(4)° were not significantly different. In the case of *o*-nitrobenzene, the presence of a proton on the carboxy group resulted in a change in this angle from 30.26(3) (COOH) to 53.88(4)° ($COO^-$), see Table 5. Clearly if just the protonation of the carboxy group results in such a large change in the angle, crystal packing forces present in **1** and **4** may be enough to account for the variances therein. Therefore, this interplanar angle, while sensitive (i.e. near co-planarity) to the size of the substituent, does not appear restricted in any other way. Finally, the degree of twist does not cause any change in the Mo–Mo atom interaction judging from the similarities in the Mo–Mo bond distance, see Table 2, a conclusion which is consistent with an earlier study which established the Mo–Mo atom bond as insensitive [3].

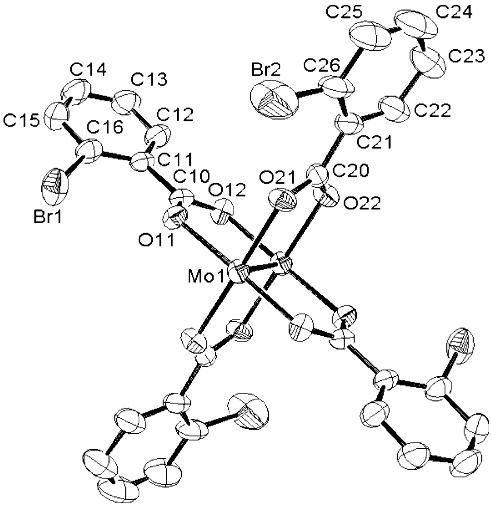

Fig. 3. ORTEP3 [22] representation of **2** displaying the atomic labeling scheme. THF molecules and H atoms were omitted for clarity. Thermal ellipsoids are drawn at the 50% probability level.

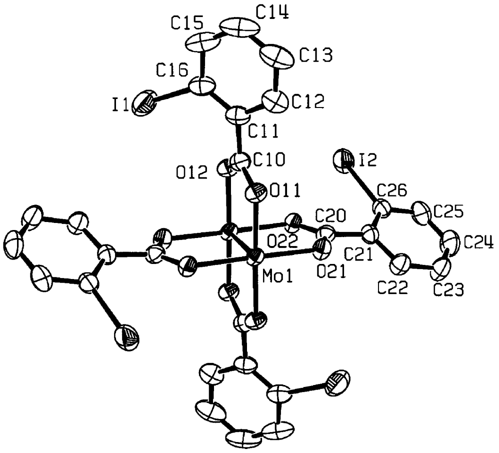

Fig. 4. ORTEP3 [22] representation of **3** displaying the atomic labeling scheme. THF molecules and H atoms were omitted for clarity. Thermal ellipsoids are drawn at the 50% probability level.

## 4. Supplementary material

Crystallographic data for the structural analysis have been deposited with the Cambridge Crystallographic Data Centre, CCDC Nos. 179597–179601 for compounds **1**–**5**, respectively, with **5** representing a redetermination of *o*-iodobenzoic acid. Copies of this information may be obtained free of charge from The Director, CCDC, 12 Union Road, Cambridge, CB2 1EZ, UK (fax: +44-1223-336-033; e-mail: deposit@ccdc.cam.ac.uk or www: http://www.ccdc.cam.ac.uk).

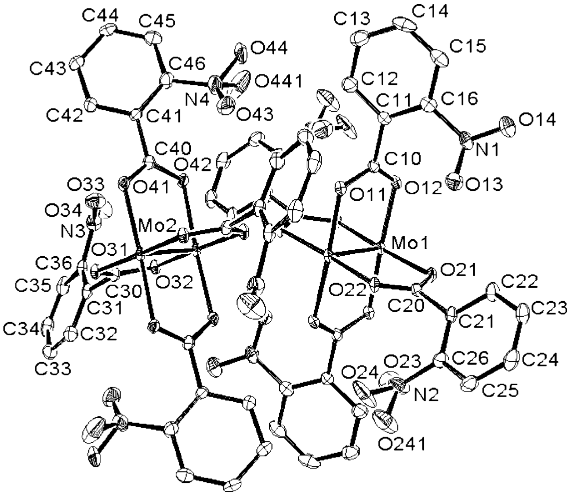

Fig. 5. ORTEP3 [22] representation of two molecules that constitute **4** displaying the atomic labeling scheme. H atoms were omitted for clarity and thermal ellipsoids are drawn at the 20% probability level.

Table 5
Comparison of selected carboxy-benzene interplanar angles and distances between *o*-halobenzoic acids and compounds **1**–**4**

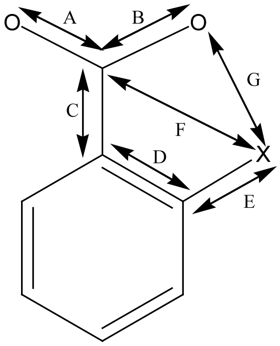

| Selected distances (Å) | *o*-Cl-benzoic acid [a] | *o*-Br-benzoic acid [b] | *o*-I-benzoic acid [c] | **1** | | **2** | | **3** | |
|---|---|---|---|---|---|---|---|---|---|
| | | | | Cl**1** | Cl**2** | Br**1** | Br**2** | I**1** | I**2** |
| A | 1.346 | 1.295 | 1.304(5) | 1.271(7) | 1.275(7) | 1.278(7) | 1.276(7) | 1.274(5) | 1.278(5) |
| B | 1.202 | 1.208 | 1.220(5) | 1.264(7) | 1.262(7) | 1.270(8) | 1.260(8) | 1.272(5) | 1.273(5) |
| C | 1.521 | 1.487 | 1.488(5) | 1.482(9) | 1.479(9) | 1.482(9) | 1.488(9) | 1.489(6) | 1.485(6) |
| D | 1.405 | 1.362 | 1.394(5) | 1.416(9) | 1.389(9) | 1.408(9) | 1.392(9) | 1.390(6) | 1.395(6) |
| E | 1.737 | 1.885 | 2.104(4) | 1.726(7) | 1.725(8) | 1.911(8) | 1.868(9) | 2.101(4) | 2.102(5) |
| F | 3.217 | 3.275 | 3.469(4) | 3.180(6) | 3.138(7) | 3.343(7) | 3.333(7) | 3.428(4) | 3.461(4) |
| G | 2.892 | 3.004 | 3.105(3) | 2.918(5) | 2.978(5) | 2.967(4) | 2.963(4) | 3.193(3) | 3.114(3) |
| Interplanar angles (°) [d] | 13.7 [a] | 18.3 [b] | 15.36(1) [e], 16.5(4) [c] | 27.5(4) | 36.4(6) | 13.8(6) | 15.1(4) | 27.9(4) | 39.4(3) |

[a] Ref. [25].

[b] Ref. [26].

[c] Ref. [27,28].

[d] For $NO_2$, interplanar angles in the free ligand are 30.26(3)° (COOH) and 53.88(4)° ($COO^-$) [29], and in **4**, 42.4(5), 64.0(5) and 52.6(5), 62.7(5)°.

[e] Ref. [28].

## Acknowledgements

We thank the Royal Thai government scholarship program (to T.L.), Michigan Technological University and the NSF (CHE-0079158) for generous support.

## References

[1] F.A. Cotton, R.A. Walton, Multiple Bonds Between Metal Atoms, second ed., Oxford, New York, 1993.
[2] F.A. Cotton, J.G. Norman, J. Coord. Chem. 1 (1971) 161.
[3] F.A. Cotton, M. Extine, L.D. Gage, Inorg. Chem. 17 (1978) 172.
[4] A. Bino, F.A. Cotton, P.E. Fanwick, Inorg. Chem. 18 (1979) 1719.
[5] F.A. Cotton, L.R. Falvello, A.H. Reid, Jr., J.H. Tocher, J. Organomet. Chem. 319 (1987) 87.
[6] F.A. Cotton, M.W. Extine, G.W. Rice, Inorg. Chem. 17 (1978) 176.
[7] F.A. Cotton, J.L. Thompson, Inorg. Chem. 20 (1981) 3887.
[8] F.A. Cotton, G.N. Mott, Inorg. Chim. Acta 70 (1983) 159.
[9] J.V. Brencic, F.A. Cotton, Inorg. Chem. 9 (1970) 351.
[10] Enraf–Nonius (1994). CAD4 express software. Enraf–Nonius, Delft, The Nethelands.
[11] A.C.T. North, D.C. Phillips, F.S. Mathews, Appl. Crystallogr., A 24 (1968) 351.
[12] A. Altomare, M.C. Burla, M. Camalli, G.L. Cascarano, C. Giacovazzo, A. Gugliardi, A.G.G. Moliterni, G. Polidori, R.J. Spagna, Appl. Crystallogr. 32 (1999) 115.
[13] L.J. Farrugia, Appl. Crystallogr. 32 (1999) 837.
[14] G.M. Sheldrick, SHELXL97, Program for Crystal Structure Refinement, University of Göttingen, Göttingen, Germany, 1997.
[15] (a) J.V. Brencic, F.A. Cotton, Inorg. Chem. 9 (1970) 351;
(b) A. Bino, F.A. Cotton, P.E. Fanwick, Inorg. Chem. 18 (1979) 1719;
(c) F.A. Cotton, L.R. Falvello, C.A. Murillo, Inorg. Chem. 22 (1983) 382.
[16] A. Carvill, P. Higgins, G.M. McCann, H. Ryan, A.J. Shiels, J. Chem. Soc., Dalton Trans., (1989) 2435.
[17] M.H. Chisholm, K.C. Glasgow, L.J. Klein, A.M. Macintosh, D.G. Peters, Inorg. Chem. 39 (2000) 4354.
[18] T. Liwporncharoenvong, R.L. Luck, J. Am. Chem. Soc. 123 (2001) 3615.
[19] D.T. Sawyer, A. Sobkowiak, Jr., J.L. Roberts, Electrochemistry for Chemists (Chapter 3), Wiley Interscience, New York, 1995.
[20] T. Liwporncharoenvong, T.B. Lu, R.L. Luck, Inorg. Chim. Acta 329 (2002) 51.
[21] J.A. Dean (Ed.), Lange's Handbook of Chemistry, 13th ed., McGraw Hill, New York, 1979.
[22] L.T. Farrugia, J. Appl. Crystallogr. 30 (1997) 565.
[23] Reference [1], p. 145.
[24] G. Ferguson, K.M.S. Islam, Acta Crystallogr. 21 (1966) 1000.
[25] (a) Data in table taken from G. Ferguson, G.A. Sim, Acta Crystallogr. 14 (1961) 1262;

(b) L. Golic, J.C. Speakman, Izv. Jug. Cent. Krist., Ser. A 10 (1975) 72.

[26] G. Ferguson, G.A. Sim, Acta Crystallogr. 15 (1962) 346.

[27] The structure of *o*-iodobenzoic acid was reported in Ref. [28]. However, this was with an *R* value of 8%. We have redetermined this structure (*R* value of 2%, submitted as supplementary material) for the purpose of getting more accurate bond lengths and angles and this is where the data reported was obtained.

[28] J.Z. Gougoutas, Cryst. Struct. Commun. 6 (1977) 703. Interplanar angle calculated using the program PARST (M. Nardelli, J. Appl. Crystallogr. 28 (1995) 659) with data from the Cambridge Data Base (CDB) (F.H. Allen, O. Kennard, R. Taylor, Acc. Chem. Res. 16 (1983) 146).

[29] G. Smith, J.M. Gentner, D.E. Lynch, K.A. Byriel, C.H.L. Kennard, Aust. J. Chem. 48 (1995) 1151. PARST [28] used to calculate angle with data from the CDB [28].